Study on a 3D-Bioprinted Tissue Model of Self-Assembled Nanopeptide Hydrogels Combined with Adipose-derived Mesenchymal Stem Cells

Guanzhou Zhou
Zibo Central Hospital
Ailing Tian
Shandong University
Lufeng Fan
Shandong University
Wenchong Shao
Shandong University
Han Wu
Shandong University
Nianfeng Sun (sunnianfeng@126.com)
Shandong University Qilu Hospital Department of Cardiology https://orcid.org/0000-0002-1997-9832

Research Article

Keywords: self-assembled nanopeptides, adipose-derived mesenchymal stem cells, 3D bioprinting, tissue engineering

Posted Date: February 19th, 2021

DOI: https://doi.org/10.21203/rs.3.rs-211896/v1

Abstract

Objective This study aimed to observe the cell growth status and multidirectional differentiation ability in a 3D-bioprinted tissue model of self-assembled nanopeptides and human adipose-derived mesenchymal stem cells (Ad-MSCs). Methods Primary Ad-MSCs were isolated, cultured, and identified by flow cytometry. Tissue models were printed via 3D bioprinting technology using a "biological ink" consisting of a mixed solution of self-assembled nanopeptides and Ad-MSCs. Ad-MSCs were induced into osteogenic, adipogenic, and endothelial differentiation and compared with the control groups by staining. Results The nanopeptide fiber was 10-30 nm in diameter and 200-500 nm in length under the atomic-force microscope. It had the characteristics of nano-scale materials. Flow cytometry showed that the isolated and cultured cells were positive for CD29 (98.51%), CD90 (97.87%), and CD166 (98.32%) but did not express CD31 (1.58%), CD34 (2.42%), CD45 (2.95%), or human leukocyte antigen (HLA)-DR (0.53%), consistent with the immunophenotype of Ad-MSCs. Then, a tissue model was printed using the biological ink, followed by induction of differentiation of Ad-MSCs within the tissue model. Alizarin red S staining showed the formation of calcium nodules in the osteogenesis induction experimental group, and oil red O stained lipid droplets in Ad-MSCs in the adipogenesis induction experimental group, whereas the two control groups were not stained. Conclusion Ad-MSCs from primary cultures have the characteristics of stem cells. Self-assembled nanopeptide hydrogel is a good tissue engineering material that can serve as an extracellular matrix. Ad-MSCs in the 3D-printed tissue model using a biological ink consisting of a mixed solution of self-assembled nanopeptides and Ad-MSCs grew well and still had strong differentiation ability.

Introduction

Stem cell differentiation is not only related to the pre-existing programming inside the cell but also regulated by the microenvironment in which the cell is located. Regulation of stem cell differentiation mainly occurs between cells and between the cell and the extracellular matrix, with cytokines fulfilling the functions of signal transduction and nutrition between cells and between the cell and the extracellular matrix. Therefore, factors affecting targeted endothelial differentiation of stem cells consist mainly of three aspects, cytokines, extracellular matrix, and microenvironment [1-2]. Zuk et al. isolated, cultured, and identified adipose tissue–derived mesenchymal stem cells (Ad-MSCs) and showed that under specific induction conditions, Ad-MSCs could differentiate into osteoblasts, chondrocytes, adipocytes, cardiac muscle cells, and endothelial cells, making them new seed cells of great interest [3-4].

Taking peptides as the basic building blocks and relying on the natural self-assembly of peptide molecules to obtain novel nanohydrogel materials has become a research hotspot in the field of tissue engineering. This type of peptide nanohydrogel has high biocompatibility and degradability plus the more prominent advantages of being biologically active and being easily compounded with different biologically active molecules according to different needs, thus carrying the feature of “bio-intelligence” [5].

In recent years, with the development of stem cell technology and 3D bioprinting technology, people have begun to explore the generation of new tissue-engineered organs through 3D bioprinting [6-7]. At present, some scientific research institutes have taken the lead in achieving 3D printing using biological materials and cells under sterile conditions. The printed human living cells have a survival rate of up to 90%. A few human tissues, such as ear cartilage tissue, liver units, and renal units, have been successfully printed [8-10].

We cultured and validated Ad-MSCs, prepared functionalized self-assembled nanopeptide hydrogels, utilized a mixed solution of Ad-MSCs and self-assembled nanopeptides as the "biological ink," and printed the tissue model using 3D bioprinting technology, thereby inducing the Ad-MSCs to undergo osteogenic and adipogenic differentiation. Lastly, the success of the model was validated.

Materials And Methods

1. Isolation, culture, and immunophenotypic identification of Ad-MSCs

1.1 Isolation, culture, and passaging of Ad-MSCs

All patients signed an informed consent form, which was approved by the hospital ethics committee. Fresh adipose tissue was cut into pieces and added to type I collagenase. After digestion, centrifugation, resuspension, and filtration, the obtained cells were added to Dulbecco's modified Eagle's medium (DMEM)/F12 complete culture medium, and the resulting P0 culture was placed in a 37 °C, 5% CO_2 incubator with saturated humidity. Cell growth and cell morphology were observed daily under an inverted phase-contrast microscope. The P0 Ad-MSCs were digested with trypsin and ethylene diamine tetraacetic acid (EDTA). The digestion was stopped when the cells became oval-shaped and the intercellular space became larger. The adherent cells were suspended, added again to DMEM/F12 complete culture medium, and inoculated into a new culture bottle at a 1:3 ratio with 10% fetal bovine serum (FBS) complete culture medium, which became the P1 culture. Cell morphology and growth were observed under an inverted phase-contrast microscope. Cells were subsequently passaged using the same method.

1.2 Immunophenotyping of Ad-MSCs

A sufficient amount of digested P3 suspension was taken and centrifuged at 1000 r/min. The cells were resuspend with 900 μl 1× phosphate-buffered saline (PBS) and distributed evenly into nine 2-ml Eppendorf tubes, to which PE mouse IgG1 20 μl, PE CD29 20 μl, PE CD31 20 μl, PE CD34 20 μl, PE CD45 20 μl, PE CD90 10 μl, PE CD166 20 μl, PE IgG2a 20 μl, and HLA-DR 20 μl were added, respectively. The Eppendorf tubes with added antibodies were incubated in the dark for 20 minutes with gentle shaking every few minutes. Cells were resuspended with PBS and then centrifuged, and this step was repeated twice to wash away the residual antibodies. The cells were finally resuspended with 500 μl 1× PBS and placed in a flow cytometry–specific tube for detection on the machine.

2. Preparation and detection of self-assembled nanopeptide hydrogel

2.1 Preparation of self-assembled nanopeptide solution

The powders of three peptides, RADA16-I, RGD, and KLT, were dissolved with biological-grade, sterile, deionized water. Their concentrations were adjusted to 10 g/L, and the mixtures underwent ultrasonic vibration for 15 minutes with an ultrasonic cell pulverizer. RADA16-I, RGD, and KLT were mixed at a volume ratio of 2:1:1, and the mixture was again mixed well by ultrasonic vibration with an ultrasonic cell pulverizer to successfully prepare a self-assembled nanopeptide mixed solution. The self-assembled nanopeptide solution was diluted to a concentration of 0.01% and was ultrasonically vibrated with an ultrasonic cell pulverizer. A small amount of this 0.01% self-assembled nanopeptide mixed solution was added dropwise onto a special mica sheet for observation of the nanopeptide fiber structure by atomic-force microscopy could.

2.2 Preparation of self-assembled nanopeptide hydrogel

The required Transwell chambers were placed in a 24-well plate and kept at room temperature overnight to allow the PBS in the 24-well plate to fully penetrate the Transwell basement membrane. The PBS solution was removed by aspiration, and the self-assembled nanopeptide mixture solution was slowly added along the edge of the Transwell chamber to replace the PBS in the 24-well plate until the surface of the PBS solution was higher than the height of the self-assembled nano-peptide mixture in the Transwell chamber. The self-assembled nano-peptide hydrogel gradually formed after standing still. The Transwell chamber was then taken out, the lower membrane of Transwell was removed, and the formed nanopeptide hydrogels were observed.

2.3 Scanning electron microscope (SEM) detection of self-assembled nanopeptide hydrogel

After following the above steps to obtain self-assembled nanopeptide hydrogel, the self-assembled nanopeptide hydrogel was fixed with glutaraldehyde fixing solution and then dehydrated. The dehydrated specimens were made into electron microscope specimens, and the internal structure of the specimens was observed under SEM.

3. Compound experiments of self-assembled nanopeptide hydrogels and Ad-MSCs

The P3 Ad-MSCs were taken, and after PBS washing, cells were added to 1 ml 0.125% trypsin-EDTA for digestion in a 37 °C incubator for 5 minutes. The flask was gently shaken, and cells were repeatedly observed under an inverted phase-contrast microscope. When the cells became spherical and the intercellular space became large, the digestion was stopped by the addition of 1 ml of DMEM/F12 complete culture medium (10% FBS), and the adherent cells were suspended by repeated pipetting to form a single cell suspension. The suspension was added to a sterile centrifuge tube and centrifuged at 1000 r/min after balancing. Cells were resuspended with 10 g/L self-assembled nanopeptide mixed solution and mixed by pipetting. The self-assembled nano-peptide hydrogel containing cells was placed into Transwell chambers, PBS was added to the 24-well plate, and DMEM/F12 complete culture medium

(10% FBS) was added to the chamber immediately after gelation. Cell morphology and growth status were observed daily under an inverted phase-contrast microscope.

4. Self-assembled nanopeptide hydrogel combined with Ad-MSCs as the biological ink for 3D-printed tissue models and induced differentiation assay of cells

4.1 Self-assembled nanopeptide hydrogel combined with Ad-MSCs as the biological ink for 3D-printed tissue models

Ad-MSCs of P2 were added to 0.125% trypsin-EDTA, digested in a 37 °C incubator, and resuspended by repeated pipetting to form a single-cell suspension. The cells were then resuspended with the 10 g/L self-assembled nanopeptide mixed solution and mixed well. The self-assembled nanopeptide solution containing Ad-MSCs was quickly added to the sterile "cartridge" of the 3D bioprinter, and the required model parameters were adjusted using the AnyPrint software on a computer to form a cylinder with a diameter of approximately 1 cm and height of approximately 5 mm, containing small cavities of different sizes. After the parameters were set, printing was started, and the substrate used for printing was 1× PBS. The printed 3D tissue model was quickly transferred to a six-well plate, added to DMEM/F12 complete culture medium (10% FBS), and placed in a 37 °C, 5% CO_2 cell incubator with saturated humidity. The morphology of the 3D tissue model was observed 24 hours later, and the state of the cells inside the model was observed under the inverted phase-contrast microscope.

4.2 Phalloidin staining of cells inside the 3D-printed tissue model

The printed tissue model was stained with phalloidin to observe the cell structure in the tissue model. After the printed tissue model was cultured for 7 days, the tissue model was washed with PBS, then sliced into paraffin sections. The sections were soaked in 0.1% Triton X-100 for 3-5 minutes and washed with PBS, and the cells were incubated with 1× PBS containing 1% BSA for 20-30 minutes. The staining solution was added dropwise to the cover glass, and the sections were stained at room temperature for 20 minutes, dried, sealed, observed under a laser confocal microscope, and stored in a dark environment.

4.3 Induction of osteogenic differentiation of cells in the 3D-printed tissue model and alizarin red S staining

The printed tissue model was cultured for 3 days, and the mesenchymal stem cell osteogenic differentiation complete culture medium was added to the six-well plate, followed by medium changes once every 3 days. After 4 weeks of induction, the tissue model was paraffin-sectioned and fixed with 4% paraformaldehyde. Alizarin red S staining solution was added dropwise, and the culture plate was placed under a microscope to observe the effect of osteogenic staining.

4.4 Induction of adipogenic differentiation of cells in the 3D-printed tissue model and oil red O staining

The printed tissue model was cultured for 3 days, and mesenchymal stem cell adipogenic differentiation medium A was added to the six-well plate. Every 3 days, this medium was alternated with adipose-derived

mesenchymal stem cell adipogenic differentiation medium B. After five switches between media A and B (approximately 20 days), cells were kept in medium B for 7 days, until the lipid droplets became large and round. After the adipogenic differentiation induction was completed, the tissue model was frozen-sectioned. Oil red O dye working solution was added dropwise to it, and the culture plate was placed under a microscope to observe the effect of adipogenic staining.

4.5 Induction of endothelial differentiation of cells in the 3D-printed tissue model and flow cytometry validation

The printed tissue model was cultured for 3 days, the cells were resuspended in endothelial cell support solution, that is, 100% EGM2-MV induction culture medium, and placed into the six-well plate. The morphological changes of the cells were observed with an inverted phase-contrast microscope every day. The medium was refreshed every 3 days, and the growth of the cells was closely observed. After 4 weeks, CD31-PE was used to label cells that had gone through induction of differentiation and those that had not undergone differentiation, and immunophenotyping was performed using flow cytometry.

Results

1. Isolation, culture, and identification of Ad-MSCs

1.1 Morphological characteristics of Ad-MSCs

Adipose tissue was diced and digested with type I collagenase. When the adipose tissue was mixed with collagenase, it mostly floated on top of the collagenase (Figure 1-1A). After centrifuging the adipose tissue, we found that the centrifuged liquid was divided into three layers: the top layer was the digested adipose tissue, the middle layer was the clear solution of type I collagenase, and the bottom layer was a mixed precipitate with mesenchymal stem cells and a small number of erythrocytes (Figure 1-1B). After 48 hours of culture, observation under the inverted phase-contrast microscope showed that there were round, nonadherent cells, dead cells, and suspended erythrocytes in the culture medium, and the bottom of the tissue culture vessel had adherent cells, which were spindle-shaped, had few cell protrusions, and were fibroblast-like (Figure 1-1C). After 5 days of culture, there were more cells than at 48 hours. However, the cells grew slowly and were long and spindle-shaped, and only few cells were triangular or irregularly shaped (Figure 1-1D). Daily observations showed that the cell growth rate gradually accelerated. On the 15th day, the degree of cell confluency was high, and the cell morphology did not change significantly, but the entire population of cells showed a swirling or school-of-fish-like growth trend (Figure 1-1E). Later subcultures showed no obvious morphological or growth changes (Figure 1-1F).

1.2 Immunophenotyping of Ad-MSCs

Flow-cytometric immunophenotyping showed that endothelial marker antibody CD31 was negative, the hematopoietic stem cell and endothelial marker antibody CD34 was negative, the leukocyte marker antibody CD45 was negative, the fibroblast marker antibody HLA-DR was negative, and the rest of the

mesenchymal stem cell marker antibodies (CD29, CD90, and CD166) were all positive, which can exclude the possibility of other cell types. Flow-cytometric phenotype identification showed that the cells that we isolated and cultured conformed to the immunophenotypic characteristics of Ad-MSCs, that is, the cells obtained from the isolation and culture were Ad-MSCs (Figure 1-2).

2. Preparation of self-assembled nanopeptide hydrogel and detection by electron microscopy

2.1 Preparation of self-assembled nanopeptide solution

The three self-assembling nanopeptides RADA16-I, RGD, and KLT are all white, powdery substances. When biological-grade, sterile, deionized water was added, the aqueous solution was initially thick and turbid. After an ultrasonic cell pulverizer was used to sonicate the viscous and turbid self-assembling nanopeptide solution, the viscous and turbid peptide solution gradually clarified to become transparent or translucent, indicating that the self-assembling nanopeptide solution had been fully dissolved and mixed. Atomic-force microscope observations showed that the nanopeptides varied in length. They were mostly 200-500 nm in length and 20-50 nm in diameter (Figure 2-1).

2.2 Preparation of self-assembled nanopeptide hydrogel

The self-assembled nanopeptide mixed solution was added to the Transwell chamber and kept in the chamber overnight, and a solid gel structure appeared in the chamber. The basement membrane of the chamber was cut off, and the hydrogel was gently removed. The hydrogel was cylindrical, colorless, and transparent, the texture was loose and brittle, and it was high in water content (Figure 2-2).

2.3 SEM detection of self-assembled nanopeptide hydrogel

The self-assembled nanopeptide hydrogel was fixed and dehydrated. SEM observation showed that the sample had a fibrous or porous like structure. The diameter of the nanofibers was approximately 20-50 nm, and the cavities were approximately 5-100 nm in size (Figure 2-3).

3. Compound experiments of self-assembled nanopeptide hydrogel and Ad-MSCs

Ad-MSCs were inoculated on the self-assembled nanopeptide hydrogel. It was found that the cells were distributed uniformly, and the cell morphology changed slightly, but the cells were in a good state of extension and were tightly connected (Figure 3).

4. Self-assembled nanopeptide hydrogels combined with Ad-MSCs as the biological ink for 3D-printed tissue models; induced differentiation assay of cells

4.1 Self-assembled nanopeptide hydrogels combined with Ad-MSCs as the biological ink for 3D-printed tissue models

After mixing the self-assembled nanopeptides with Ad-MSCs and performing 3D printing, the 3D-printed tissue engineering model was a transparent cylinder approximately 1 cm in height and approximately 5

mm in diameter. It had a predesigned porous structure to promote the full contact and material exchange between cells and the culture medium as well as the proliferation, differentiation, and signaling of Ad-MSCs in the 3D-printed tissue model. The materials we used could be printed by a 3D printer, but the printed model was not a regular cylinder in shape, suggesting that the plasticity was slightly poor (Figure 4-1).

4.2 Phalloidin staining of cells in the 3D-printed model

There are many choices of immunofluorescent dyes for immunostaining the printed model. Here, we used phalloidin staining to observe the macroscopic structure of cells in the tissue model, which should have the same effect as other fluorescent dyes. After staining, we found that the cells were in a good growth state, were arranged tightly and orderly, and were in close contact with the model. The porous structures in the model let the cells fully contact the culture medium (Figure 4-2).

4.3 Induced osteogenic differentiation of cells in the 3D-printed model and Alizarin Red S staining

After inducing osteogenic differentiation of cells in the 3D model, sectioning of paraffin-embedded samples, and staining, observation under the microscope revealed that the cells were still closely packed and ordered, and dark-brown calcified nodules appeared in the cells, whereas no obvious staining was seen in the control group. These findings suggest that the induction of osteogenic differentiation and staining in the 3D-printed tissue model were successful (Figure 4-3).

4.4 Induction of adipogenic differentiation and oil red O staining of cells in the 3D-printed model

After inducing adipogenic differentiation of cells in the 3D model, sectioning of paraffin-embedded samples, and staining, observation under the microscope revealed that the cells were still arranged tightly and orderly, and there were many lipid droplets in the cells, seen as round, red bubbles, but no obvious staining was seen in the control group. This shows that the induction of adipogenic differentiation and staining in the 3D-printed tissue model was convincing (Figure 4-4).

4.5 Induction of endothelial differentiation in 3D-printed tissue models and flow-cytometric identification

After inducing endothelial differentiation of cells in the 3D model, we found that the spindle-shaped cells became shorter, cells presented polygonal or triangular-like changes, and they showed an overall paving stone–like growth, whereas there was no obvious morphological change in the control group (Figure 4-5A). Flow-cytometric immunophenotyping was performed on the stem cells after induction of endothelial differentiation. After labeling, cells were loaded into the flow cytometer, and it was found that the labeling with endothelium-specific antibody CD31 changed from negative to positive, whereas the control group still had negative CD31 labeling (Figure 4-5B, C).

Discussion

Ad-MSCs have the characteristics of easy culture, strong proliferation ability, and low immunogenicity, offering great possibilities for allogeneic transplantation and an excellent source of seed cells [11]. Ad-MSCs also have the most critical ability of stem cells, that is, multidirectional differentiation ability. Under different induction conditions, Ad-MSCs can differentiate into different types of cells, such as osteoblasts, adipocytes, cardiomyocytes, chondrocytes, endothelial cells, and nerve cells. Therefore, Ad-MSCs, as an emerging type of seed cell, have good prospects in the field of regenerative medicine.

In this study, we isolated and cultured a certain number of Ad-MSCs from adipose tissue for passaging and expansion. Observation of the morphological structure revealed that the cells were spindle-shaped or showed fibroblast-like changes, and the entire population showed a swirling or school-of-fish-like growth state. The growth rate of the P0 generation of cells was slow. After passaging, the growth rate of Ad-MSCs gradually increased until it mostly stabilized at P3.

The immunophenotypes for CD29, CD31, CD34, CD45, CD90, CD166, and HLA-DR were typed in this study. CD31 is an endothelial cell–labeling antibody, CD34 is a hematopoietic stem cell– and endothelial cell–labeling antibody, CD45 is a leukocyte-labeling antibody, and HLA-DR is a fibroblast-labeling antibody. Staining using these four antibodies was negative in our study, showing that the isolated and purified cells were not the above cell types. In contrast, CD29, CD90, and CD166 are antibodies labeling Ad-MSCs, and they all showed positive staining in our study, indicating the characteristics of stem cells and showing that our culture had the immunophenotype of Ad-MSCs.

Self-assembled nanopeptides can be transformed from a liquid state to a solid hydrogel structure under specific induction and stimulation conditions, forming many nanofibers [12]. Self-assembled nanopeptide hydrogels have great advantages in medical research: (1) they are synthesized from natural amino acids under artificial conditions and can be produced in large quantities; (2) these nanopeptides have good biocompatibility, can be degraded into natural amino acids and absorbed by the human body, and have no toxic and side effects; (3) they can be combined with active peptide fragments with different functions to construct new functionalized self-assembled nanopeptide hydrogels [13].

As an extracellular matrix, tissue-engineered materials are of great significance to cell viability [14-16]. The nanopeptide used in this study was a mixture of three peptides of RADA16-I, RGD, and KLT. After RADA16-I forms a solid-phase hydrogel, the hydrogel contains many pores inside, which is suitable for cell adhesion and migration and beneficial to nutrient transportation. KLT is a vascular growth factor polypeptide fragment that stimulates vascular endothelial growth factor receptors and promotes endothelial cell proliferation [17]. RGD is a repetitive peptide motif of cell adhesion growth factor and a key binding site for cell adhesion [18,19] that can promote the adherent growth of cells. Observing the dehydrated self-assembled nanopeptide hydrogel with an SEM revealed that the microstructure in the gel was made of an ordered intertwined porous scaffold structure, the diameter of the nanofibers was approximately 20-50 nm, the pore size was approximately 5-100 nm, and the pores accommodated Ad-MSCs.

We prepared the functionalized self-assembled nanopeptide hydrogel combined with Ad-MSCs for 3D culture. Observation with an inverted phase-contrast microscope showed the same things that SEM of the hydrogel alone did. Ad-MSCs tightly adhered to the polypeptide scaffold and presented a 3D structure. From the above, it is not difficult to see that the functionalized self-assembled peptide hydrogel has the function of an extracellular matrix and can provide cells with a more suitable microscopic environment for survival, promote cell growth, and maintain cell viability.

With the rapid development of cell biology, materials science, and 3D printing technology, 3D bioprinting has received increasing attention in the field of cultivation and repair of tissues and organs. The concept of “cell printing” was proposed by Boland et al. in 2003 [20,21], and 3D bioprinting has been used for the generation and transplantation of certain tissues and organs in the field of regenerative medicine, as well as in the fields of pharmacology and toxicology [22-24].

In the study, we first prepared the biological ink using the mixed solution of self-assembled nanopeptides and Ad-MSCs, then added the biological ink into the sterile cartridge of the 3D bioprinter and printed and stacked the solution layer by layer using PBS as the substrate. The printed 3D model was roughly cylindrical, with a diameter of approximately 1 cm and a height of approximately 0.5 cm. There were several small holes in it, which was of great significance for the exchange of substances between cells and the surrounding environment. We conducted 3D culture of Ad-MSCs in the printed tissue model. Fluorescent staining with phalloidin showed that the overall arrangement of the cells was tight and orderly, the growth was good, and the adherence of cells was tight. The cells in the printed tissue model were induced to differentiate and stained accordingly. The cells were stained, indicating that Ad-MSCs still grew normally in the 3D-printed tissue model, and there was still a strong differentiation phenomenon after appropriate induction.

We used Ad-MSCs as seed cells in this study because they have many advantages, such as easy availability and low immunogenicity. Self-assembled nanopeptides are used to support cell growth and play the role of extracellular matrix. Ad-MSCs in the 3D-printed tissue models using a mixed solution of self-assembled nanopeptides and Ad-MSCs as the biological ink showed good growth status and still had strong differentiation ability.

List Of Abbreviations

adipose-derived mesenchymal stem cells (Ad-MSCs)

human leukocyte antigen (HLA)

dulbecco's modified Eagle's medium (DMEM)

ethylene diamine tetraacetic acid(EDTA)

fetal bovine serum (FBS)

phosphate-buffered saline (PBS)

scanning electron microscope (SEM)

Declarations

Acknowledgements

The authors would like to express their gratitude to Dr. Jianmin Ling for their assistance in performing the experiments.

Funding

This study was supported by grants from the Natural Science Foundation of Shandong Province (ZR2017MH072); the Natural Science Foundation Program of Shandong Province (2016GSF201219); and Livelihood Technology Project of Qingdao(18-6-1-90-nsh).

Data Availability Statement

The data that support the findings of this study are available from the corresponding author upon reasonable request.

Authors' contributions

Zhanao Liu performed the experiments, analyzed and interpreted the data, and wrote the manuscript. Tian Ailing, Fan Lufeng; Shao Wenchong and Wu Han performed the analysis and interpretation of the data. Sun Nianfeng designed the study and revised the manuscript. All authors read and approved the final manuscript.

Ethics statement

The procedures and participation/tissues of human in this study were carried out in accordance with the National Institutes of Health (NIH) Guidelines for the Care and Use of Laboratory.

All experimental protocols were approved by the Ethics Committee of Shandong Academy of Medical Sciences.

All participants provided a statement of written informed consent.

Consent for publication

All authors of this manuscript agreed to publication.

Competing interests

The authors declare that they have no competing interests.

References

1. Chen T, Chen D, Li F, Tan Z. Netrin-1 with stem cells promote angiogenesis in limb ischemic rats. J Surg Res. 2014;192(2):664-9.
2. Rosa S, Praqa C, Pitrez P.R, Gouveia P.J, Aranguren X.L, Ricotti L, Ferreira L.S. Functional characterization of iPSC-derived arterial- and venous-like endothelial cells. *Sci Rep.* 2019, *9:* 3826-32.
3. Minonzio G, Corazza M, Mariotta L, Gola M, Zanzi M, Gandolfi E, De Fazio D, Soldati G. Frozen adipose-derived mesenchymal stem cells maintain high capability to grow and differentiate. Cryobiology. 2014; 69(2): 211-6.
4. Shojaei S, Tafazzoli-Shahdpour M, Shokrgozar MA, Haghighipour N. Effects of mechanical and chemical stimuli on differentiation of human adipose-derived stem cells into endothelial cells. Int J Artif Organs. 2013; 36(9): 663-73.
5. Liu X, Wang X, Horii A, Wang X, Qiao L, Zhang S, Cui FZ. In vivo studies on angiogenic activity of two designer self-assembling peptide scaffold hydrogels in the chicken embryo chorioallantoic membrane. Nanoscale. 2012;4(8):2720-7.
6. Moroni L, Boland T, Burdick JA, De Maria C, Derby B, Forgacs G, Groll J, Li Q, Malda J, Mironov VA. Biofabrication: a guide to technology and terminology. *Trends Biotechnol.* 2018, *36,* 384-402.
7. Moroni L, Burdick JA, Highley C, Lee SJ, Morimoto Y, Takeuchi S, Yoo J. Biofabrication strategies for 3D in vitro models and regenerative medicine. *Rev. Mater.* 2018, *3*, 21-37.
8. Byambaa B, Annabi N, Yue K, Santiago GTD, Alvarez MM, Jia W, Kazemzadeh-Narbat M, Shin SR, Tamayol A, Khademhosseini A. Bioprinted osteogenic and vasculogenic patterns for engineering 3D bone tissue. *Health Mater.* 2017, *6,*1700-15.
9. Choi YJ, Jun YJ, Kim DY, Yi HG, Chae SH, Kang J, Lee J, Gao G, Kong JS, Jang J. 3D cell printed muscle construct with tissue-derived bioink for the treatment of volumetric muscle loss. *Biomaterials.* 2019, *206,*160-169.
10. Wang K, Lin RZ, Melero-Martin JM. Bioengineering human vascular networks: trends and directions in endothelial and perivascular cell sources. *CMLS.* 2019, *76,* 421-
11. A. Zuk, M. Zhu, H. Mizuno, J. Huang, J.W. Futrell, A.J. Katz, P. Benhaim, H.P. Lorenz, M.H. Hedrick, Multilineage cells from human adipose tissue: implications for cell-based therapies, Tissue engineering, 7 (2001) 211-228.
12. Zhang, F. Gelain, X. Zhao, Designer self-assembling peptide nanofiber scaffolds for 3D tissue cell cultures, Seminars in cancer biology, 15 (2005) 413-420.
13. Yuan L, Liang P, Structural characteristics and advantages of a self-assembled peptide nanofiber scaffolds. China Tissue Chinese Journal of Tissue Engineering Research, 17 (2013) 5379-5386.
14. Gelain, D. Bottai, A. Vescovi, S. Zhang, Designer self-assembling peptide nanofiber scaffolds for adult mouse neural stem cell 3-dimensional cultures, PloS one, 1 (2006) e119.
15. Liu, X. Wang, X. Wang, H. Ren, J. He, L. Qiao, F.Z. Cui, Functionalized self-assembling peptide nanofiber hydrogels mimic stem cell niche to control human adipose stem cell behavior in vitro, Acta

biomaterialia, 9 (2013) 6798-6805.
16. H. Park, H. Cho, E.S. Gil, B.B. Mandal, B.H. Min, D.L. Kaplan, Silk-fibrin/hyaluronic acid composite gels for nucleus pulposus tissue regeneration, Tissue engineering. Part A, 17 (2011) 2999-3009.
17. Wang, M. Zhao, S. Li, U.J. Erasquin, H. Wang, L. Ren, C. Chen, Y. Wang, C. Cai, "Click" immobilization of a VEGF-mimetic peptide on decellularized endothelial extracellular matrix to enhance angiogenesis, ACS applied materials & interfaces, 6 (2014) 8401-8406.
18. Hersel, C. Dahmen, H. Kessler, RGD modified polymers: biomaterials for stimulated cell adhesion and beyond, Biomaterials, 24 (2003) 4385-4415.
19. Ruoslahti, RGD and other recognition sequences for integrins, Annual review of cell and developmental biology, 12 (1996) 697-715.
20. C. Wilson, Jr., T. Boland, Cell and organ printing 1: protein and cell printers, The anatomical record. Part A, Discoveries in molecular, cellular, and evolutionary biology, 272 (2003) 491-496.
21. Boland, V. Mironov, A. Gutowska, E.A. Roth, R.R. Markwald, Cell and organ printing 2: fusion of cell aggregates in three-dimensional gels, The anatomical record. Part A, Discoveries in molecular, cellular, and evolutionary biology, 272 (2003) 497-502.
22. Huh, B.D. Matthews, A. Mammoto, M. Montoya-Zavala, H.Y. Hsin, D.E. Ingber, Reconstituting organ-level lung functions on a chip, Science (New York, N.Y.), 328 (2010) 1662-1668.
23. Sonntag, N. Schilling, K. Mader, M. Gruchow, U. Klotzbach, G. Lindner, R. Horland, I. Wagner, R. Lauster, S. Howitz, S. Hoffmann, U. Marx, Design and prototyping of a chip-based multi-micro-organoid culture system for substance testing, predictive to human (substance) exposure, Journal of biotechnology, 148 (2010) 70-75.
24. Gunther, S. Yasotharan, A. Vagaon, C. Lochovsky, S. Pinto, J. Yang, C. Lau, J. Voigtlaender-Bolz, S.S. Bolz, A microfluidic platform for probing small artery structure and function, Lab on a chip, 10 (2010) 2341-2349.

Figures

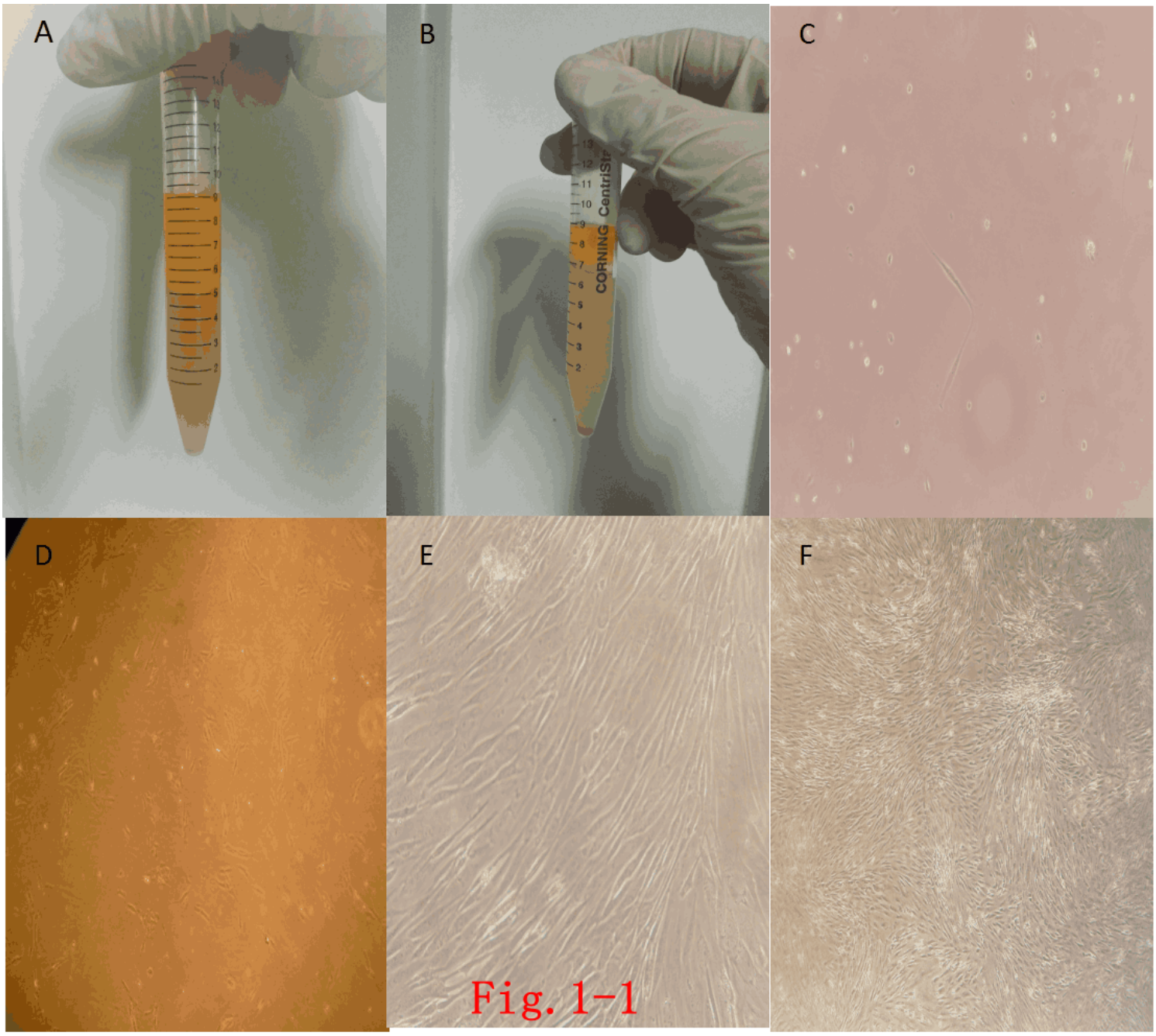

Figure 1

Fat digestion and morphology of Ad-MSCs A: Fat mixed with type I collagenase. B: Complete digestion of fat by type I collagenase and centrifugation. C: Primary Ad-MSCs at 48 h (× 200). D: Ad-MSCs at 5 d (× 100). E: Ad-MSCs at 15 d (× 100). F: P2-generation Ad-MSCs (× 40).

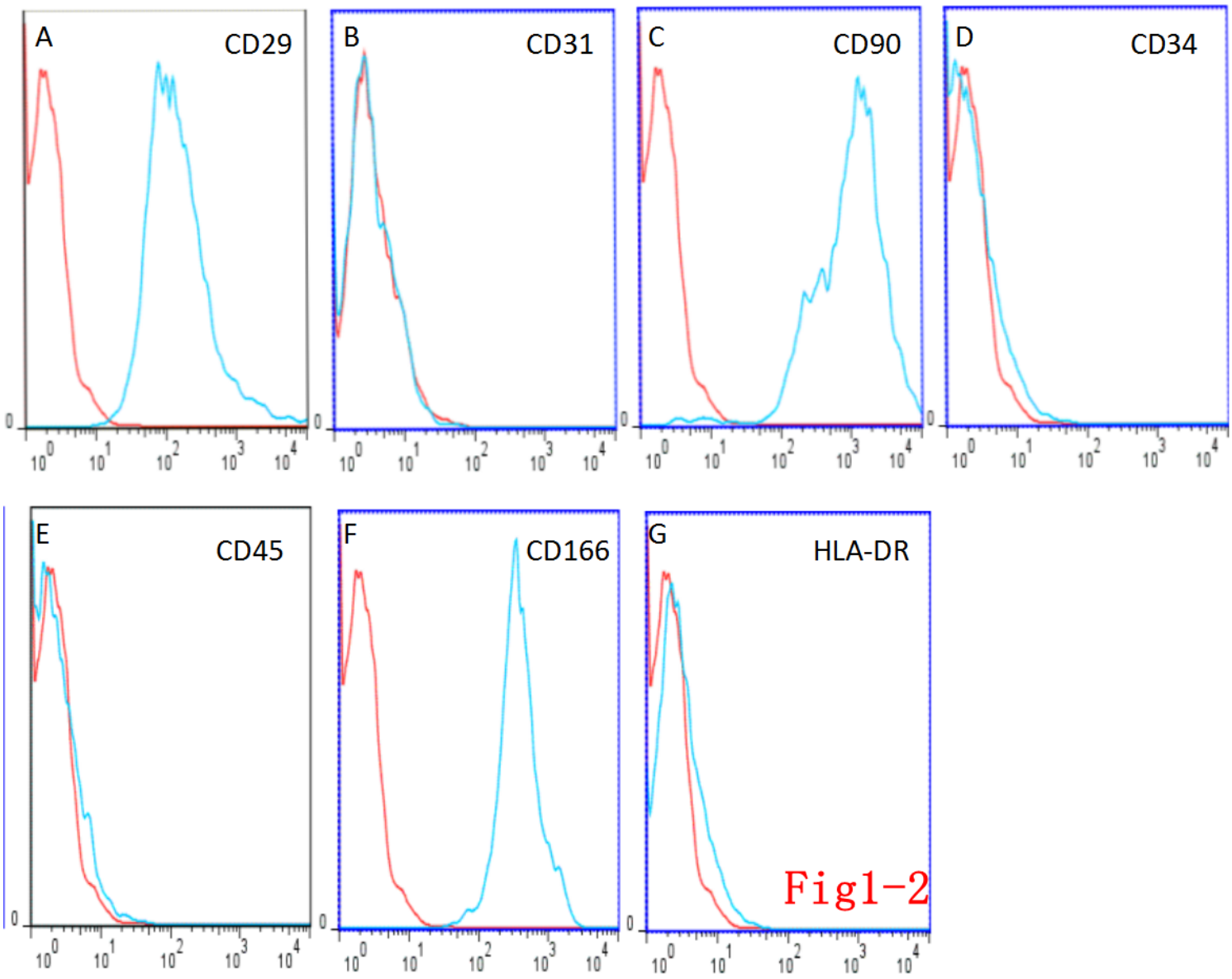

Figure 2

Ad-MSC immunophenotyping A: CD29-positive expression. B: CD31-negative expression. C: CD90-positive expression. D: CD34-negative expression. E: CD45-negative expression. F: CD166-positive expression. G: HLA-DR-negative expression.

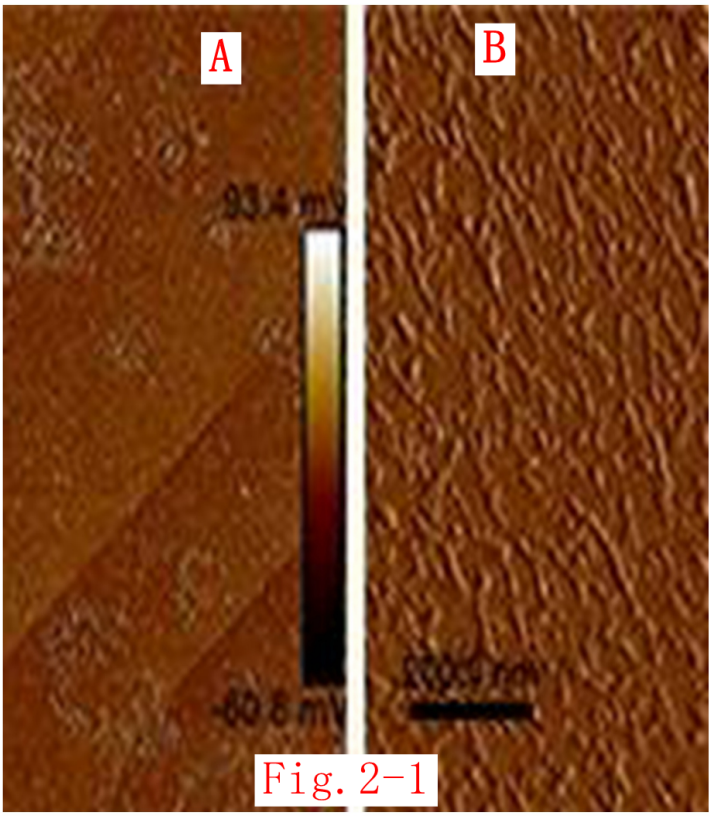

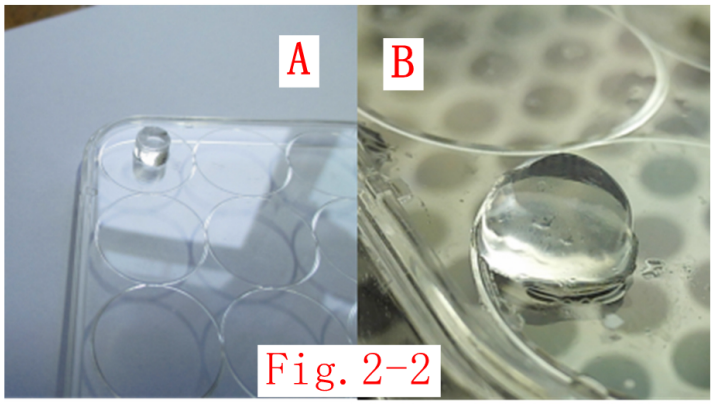

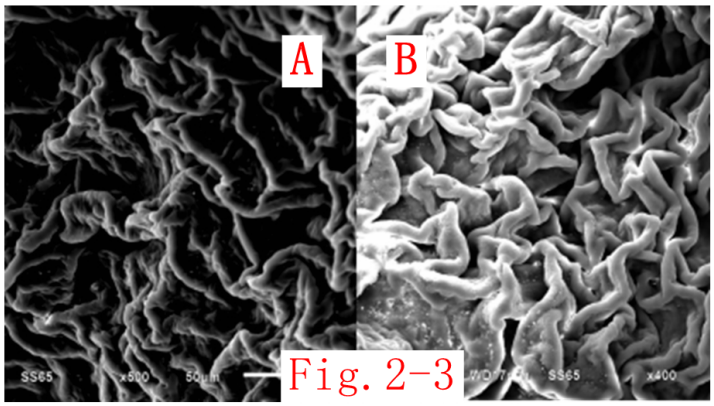

Figure 3

Atomic-force microscope image of self-assembled nanopeptide solution: A: The nanofiber arrangement can be seen by imaging for the three-peptide mixed solution at 2.0 μm. B: The nanofiber arrangement can be seen by imaging for the three-peptide mixed solution at 200 nm. Figure 2-2. Image of gelation of the nanopeptide solution through the Transwell chamber: A: Observation of the nanopeptide hydrogel structure from a long distance (the bottom plate is a 12-well plate). B: Observation of the nanopeptide hydrogel structure from a close distance (the bottom plate is a six-well plate). Figure 2-3. SEM observation of the nanopeptide hydrogel: A, B: SEM observation of the nanopeptide hydrogel shows that its microstructure is tightly arranged, with pores that can accommodate cells (50 μm).

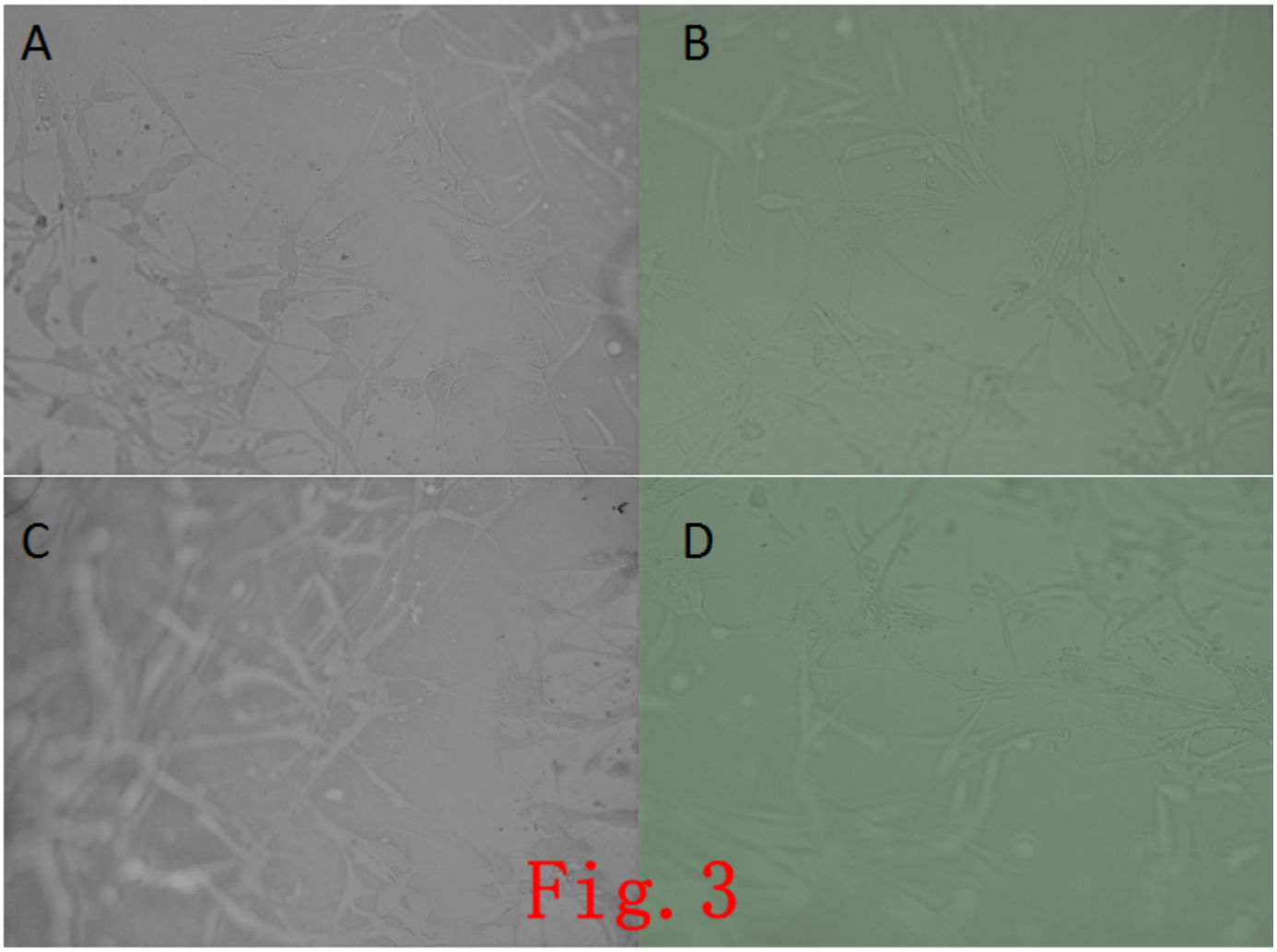

Figure 4

Observation of cells in a self-assembled the nanopeptide hydrogel model combined with Ad-MSCs A, B, C, D: Images of cells in the hydrogel photographed at different angles, showing that the cells in the hydrogel have a good growth condition with good adherence (×100).

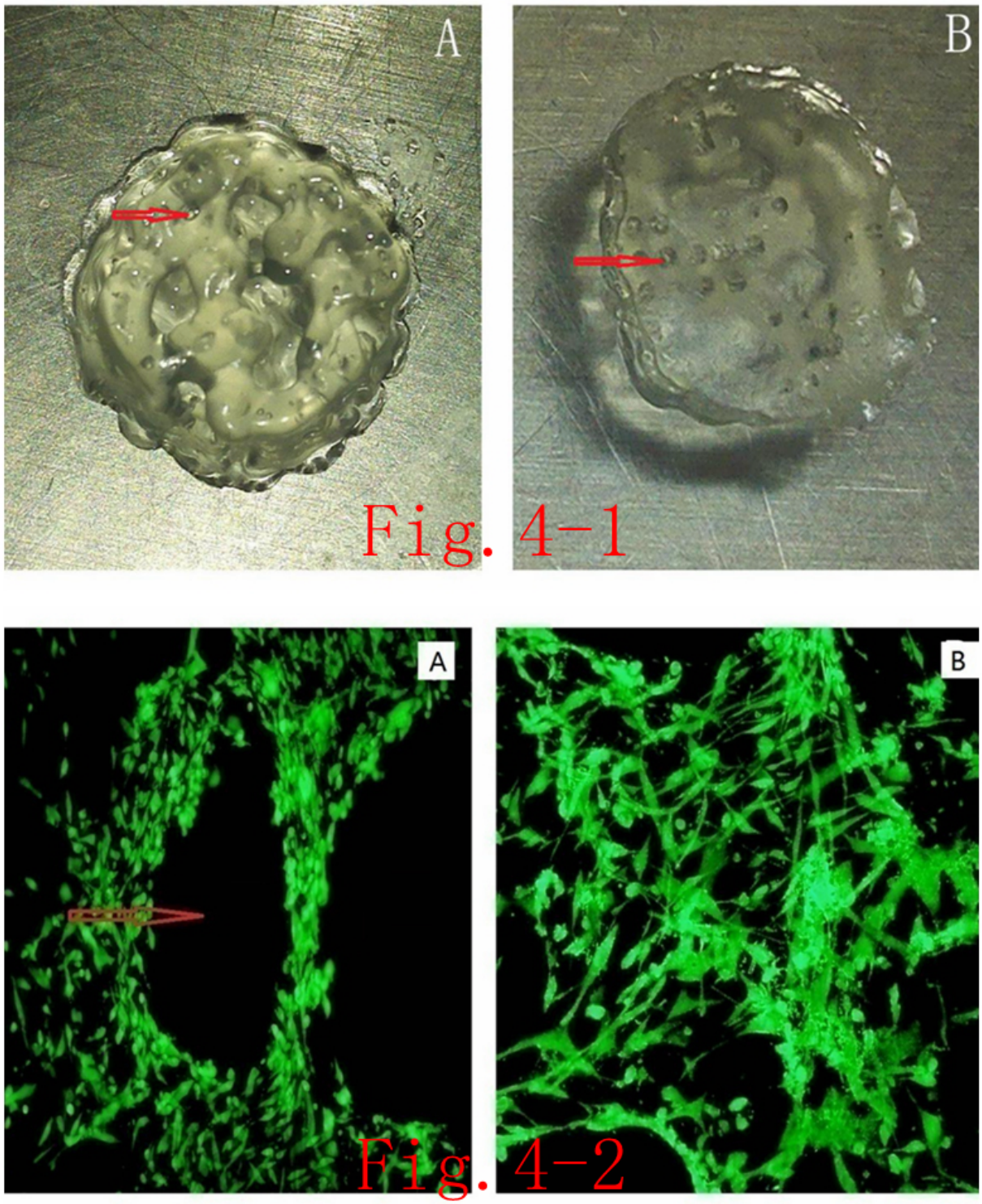

Figure 5

3D-printed tissue model based on self-assembled nanopeptides and Ad-MSCs: A: Front side of the 3D-printed model, revealing that it is not a regular cylindrical structure and there are pore-like structures as designed by the software. The red arrow in the figure points to the pore (the diameter of the cylinder is 1 cm). On the reverse side of the 3D model, a pore-like structure is still visible (the diameter of the cylinder is 1 cm). Figure 4-2. Phalloidin staining of cells in a 3D-printed tissue model: A: After the 3D-printed model

was sectioned and stained, the internal structure was observed by fluorescence microscopy. Red arrows point to pore-like structures (×40). B: After the 3D-printed model was sectioned and stained, fluorescence microscope observation of the interval structure shows that the cells are arranged in an intricate and tight manner (×40).

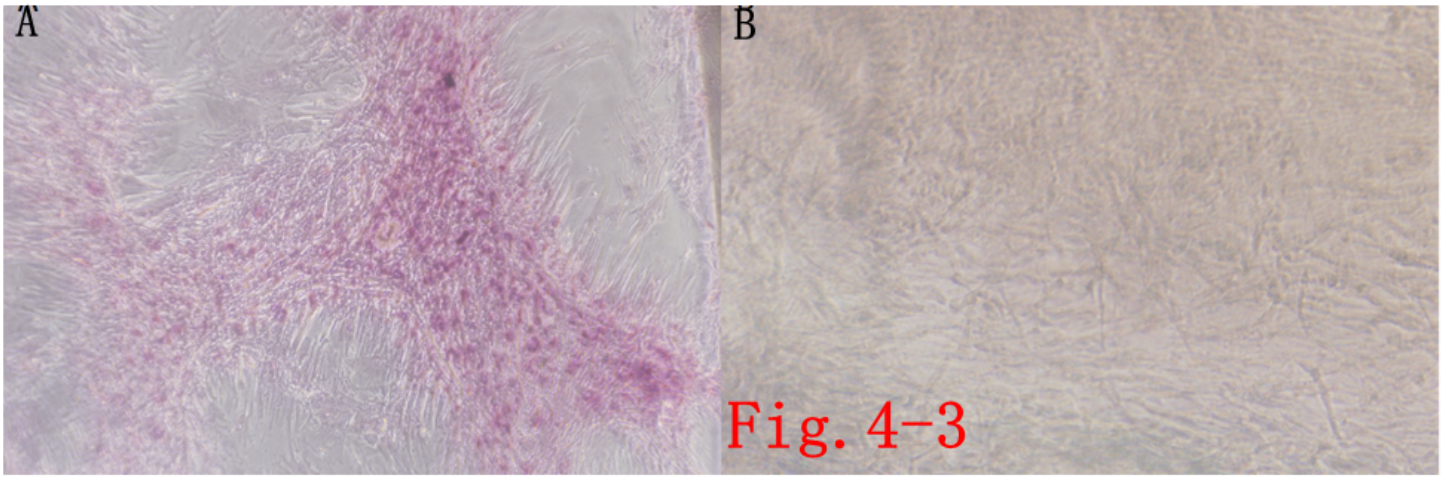

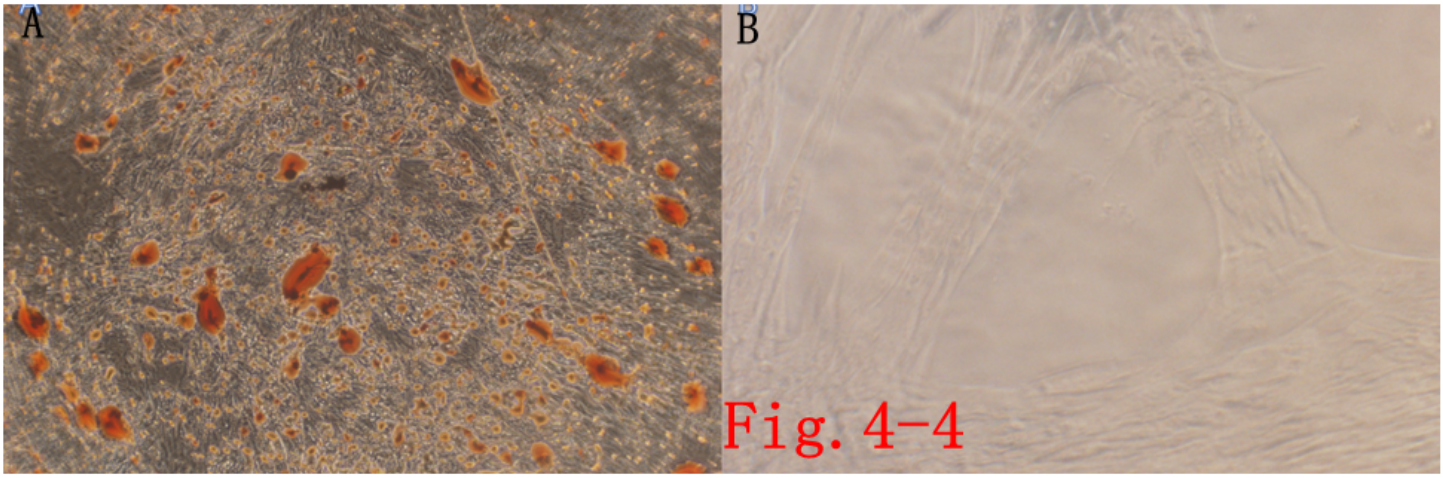

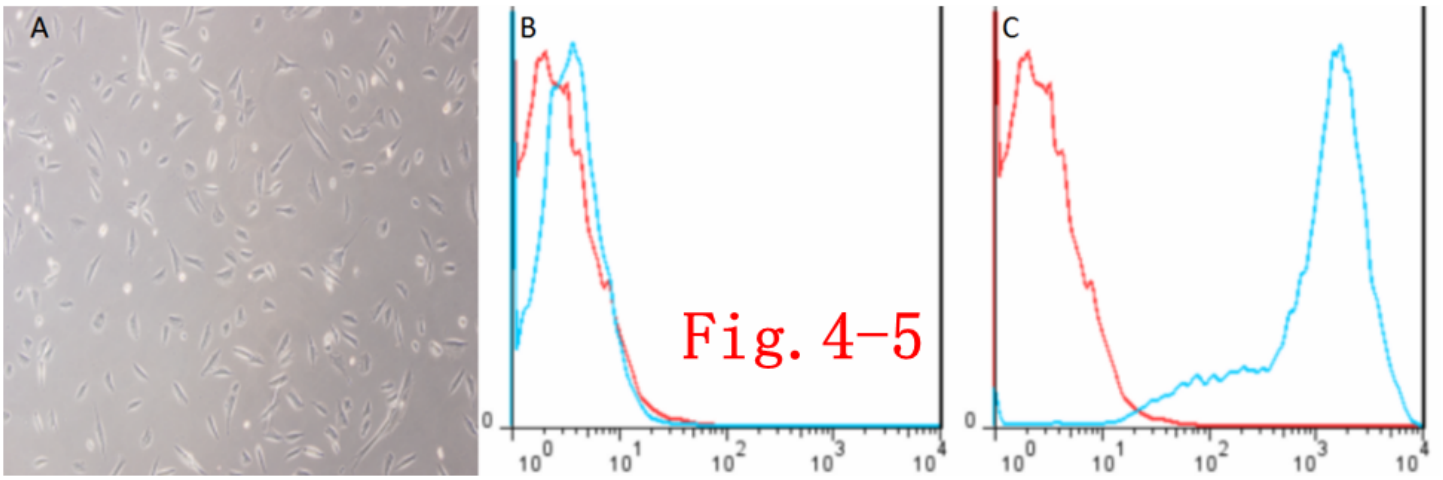

Figure 6

Alizarin red S staining after osteogenic induction of cells in the 3D-printed model: A: Alizarin red S staining was performed on the Ad-MSCs in the 3D-printed models after osteogenic differentiation and

sectioning. Cells were densely packed with red calcium nodule precipitation (×40). B: The model without induction of differentiation. Ad-MSCs show no obvious staining (×40). Figure 4-4. Oil red O staining of cells in the 3D-printed model after adipogenic differentiation: A: After adipogenic differentiation of Ad-MSCs in the 3D-printed model, oil red O staining was performed after sectioning. Red lipid droplets are seen in the cells (×40). B: Oil red O staining on cells in the models with no adipogenic differentiation. No obvious staining is seen (×100). Figure 4-5. Induced endothelial differentiation of cells in the 3D-printed model and immunophenotyping via flow cytometry: A: Induction of endothelial differentiation of Ad-MSCs in the 3D-printed model. Cells demonstrate paving stone–like changes (×100). B: CD31-negative expression in the control group. C: CD31-positive expression in the experimental group.